وزارة
التعليم العالي والبحث العلمي
جامعة ميسان
كلية التربية الاساسية

مجلة ميسان للدراسات الاكاديمية

مجلة ميسان للدراسات الأكاديمية

للعلوم الانسانية والاجتماعية والتطبيقية

Misan Journal For Academic Studies Humanits, Social and applied Sciences

ISSN (Print) 1994-697X

(Online)-2706-722X

المجلد 25 العدد 58 حزيران 2026

25 vol 58 Issue 2026 June

مجلة ميسان للدراسات الاكاديمية
العلوم الانسانية والاجتماعية والتطبيقية
كلية التربية الاساسية/ جامعة ميسان

المجلد 25 العدد 58 حزيران 2026

VOLE 25 SSUE 58 ,2026 JUNE

رقم الايداع في المكتبة الوطنية العراقية 1326 لسنة 2009

journal.m.academy@uomisan.edu.iq
https://www.misan-jas.com/index.php/ojs
https://iasj.rdd.edu.iq/journals/journal/view/298

MISAN JOURNAL FOR ACADEMIC STUDIES
HUMANITS, SOCIAL AND APPLIED SCIENCES
VOLE 25 ISSUE 58 JUNE,2026
MJAS

ت	فهرس البحوث	الصفحة
1	The impact of social, economic and health factors on the employment of the elderly in the center of Amara district Wisam A. Dargal	18 -1
2	Designing drugs by molecular docking to inhibit COVID-19 Abbas Kareem , Bahjat A. Saeed	40 - 19
3	Hexagonal Boron Nitride synthesis, its applications in dentistry and cytotoxicity: A literature review Al-Safa Malik Jaseim , Faiza Mohammed Hussain Abdul-Ameer	53 - 41
4	Racial Capitalism and the Architecture of Captivity in Colson Whitehead's The Underground Railroad Ibraheem Ajeel Dakhil	74 - 54
5	The Relationship between Linguistic Intelligence and Academic Achievement in Reading Comprehension among Students of English Department Dijla Abbood Shareef Al-Turfi	88 - 75
6	Sea Wave Energy Estimating in front of the Iraqi Coast, Northwest Arabian Gulf Adel Jassim Al-Fartusi , Sajjad k. Chasib	97 - 89
7	Reservoir Property Evaluation of the Mishrif Formation Using Integrated Petrophysical Analysis, West Qurna-1 Oilfield Zahraa Sh . Al-Maliki , Muwafaq F. Al –Shahwan	107 - 98
8	The Role of Molecular Biology in Cancer Treatment: Advances, Applications, and Future Perspectives Ali Isam Najm	115 - 108
9	Study of Morphometric Tectonic Indicators of the Wadi Al-Hay Basin in the Najaf desert using GIS data Latif Jabbar Farhan	127 - 116
10	Environmental Assessment of the Water of Haditha Dam and Reservoir for the Period (2023–2024) Using the Canadian Water Quality Index (CCME-WQI) Rajaa Kadhim Mutar	140 - 128
11	The Extent of Primary School Mathematics Teachers' Knowledge of Constructivist Teaching Skills from Their Perspectives Noor Ali Abdul Karim , Anwar Sabah Abdul-Majid	161 - 141
12	The Effectiveness of Teaching Based on Visual Interpretive Thinking in Developing Aesthetic Awareness among Art Education Students Mohsin Hameed Malik	181 - 162
13	Problems of Reliance on Lexicons in Linguistic Criticism: A Diachronic Study Murtadha Hamdan Ajib	198 - 182
14	The Integration of Artificial Intelligence and Public Relations:An Analytical Study of AI Use in Communication Messages to thePublic Aqeel Tahseen Fathallah , Ali Muhanad Hamid , Osama Kareem Rasheed	214 - 199

232 - 215	Mechanisms of domination and representations of resistance in contemporary Libyan narrative: A cultural approach to Najwa Bin Shatwan's novel, (Slave Pens). Raad Huwair Sweilem	**15**
243 - 233	logical analysis of the skeptical concept of faith Jabbar Nasser Yousef	**16**
260 - 244	The United States' Entry into World War I and Its Impact on U.S -Canadian Relations (1917-1918). Jawad Kadhim Dakhil , Ammar Khalid Ramadan	**17**
268 - 261	The Relationship Between Image Reading Skills and Visual Perception Among Students of the Art Education Department Fatima Jabbar Hussein	**18**
287 - 269	The significance of Ilm al-Rijāl and its connection with the Hadith sciences. Abbas Jassim Nasser	**19**
308 - 288	The Effectiveness of the Think Silently Strategy on Academic Achievement and Science Process Skills among First-Grade Intermediate Students in Biology Ali Jabbar Yaseen	**20**
328 - 309	Performance in Contemporary Plastic Art ,as an Evolutionary Manifestation of Perspectival Representation Zahraa Mahood Mohammad	**21**
359 - 329	Future Thinking and Professional Agency as Predictors of Academic Transition Shock among Newly Appointed University Instructors Seenaa Ahmed Ali	**22**
371 - 360	The Effect of an Educational Program Based on the Van Hiele Model on Developing Visual Culture of Contemporary Arts among Students of the Art Education Department Hussein Rishk Khdier	**23**
394 - 372	Geographical Factors and Their Impact on the Cultivation of Field Crops in Misan Governorate Sahar Rami Eidan	**24**
416 - 395	Intellectual Reform in the First Hijri Century (The Protest of the Companions in Defense of the Legitimacy of the Caliphate of Imam Ali Ibn Abi Talib (peace be upon him) in 11 AH/632 CE as a Model) Fatima Abd Saeed Al-Maliki	**25**

ISSN (Print) 1994-697X
ISSN (Online) 2706-722X

DOI: https://doi.org/10.54633/2333-025-058-002

Received:26,June,2025
Accepted:19,July,2025
Published online:30/June/2026

MJAS: Humanities, Social and Applied Sciences
Publishers
The university of Misan.
College of Basic Education

Designing drugs by molecular docking to inhibit COVID-19

Abbas Kareem [1] , Bahjat A. Saeed [2]
Department of Chemistry, College of Education for Pure Sciences, Basrah University, Basrah, Iraq
Corresponding Anthor Email:
pgs.abbas.kareem@uobasrah.edu.iq
orcid ID: 0009-0000-5265-6114

Abstract:

The current coronavirus (COVID-19) pandemic has raised the profile of the new generation SARS-CoV-2 virus as a global health threat and its massive spread to every corner of the world has raised major concerns about the public healthcare system due to the lack of effective and reliable treatments. Therefore, it is necessary to use all possible methods to design new drugs and vaccines to reduce the disease. In this study, we designed eight Emmdpd ,Favlplravir, Hydroxychloroquine and Kifunensine -derived molecules and examined their biological potential to inhibit the main protease (Mpro) of SARS-CoV-2 through computational studies, Density Function Theory (DFT) calculations were performed on the studied compounds. Which improved the geometric structure of the compounds, The geometrically optimized structures were subjected to molecular docking calculations using the SARS-CoV-2 major protease Protein Database ID 6LU7 , Compounds 4h, 6b, 9f and 14h showed favorable pharmacological properties suitable for human use.

Keywords: COVID-19, SARS-CoV-2, Molecular docking, Emmdpd ,Favlplravir, Hydroxychloroquine , Kifunensine

1- introduction:

In 2019, the coronavirus (SARS-CoV-2) emerged and was identified as the causative agent of the COVID-19 pandemic (Pal et al. 2020) (Collins et al. 2021). Specialists first discovered the virus in Wuhan, China, and have since declared it a global pandemic (Baig et al. 2020) .Scientists have yet to discover a medicine or vaccine to prevent COVID-19 infection, necessitating the development of antiviral treatments to inhibit SARS-CoV-2 transmissio (Li and De Clercq 2020) (Demsa et al. 2021) .

SARS-CoV and SARS-CoV-2 share a striking similarity, and both are beta-coronaviruses that cause severe acute respiratory syndrome (SARS), and both cause fatal diseases in humans due to their transmission. (Buonaguro et al. 2020) . Consequently, numerous laboratories have focused on targeting the virus's structural components, including the spike glycoprotein (S), nucleoprotein envelope (N), membrane protein (M), and envelope protein (E) (Elfiky 2020) . The coronavirus major protease Mpro and RNA-dependent RNA polymerase (RdRp) are needed for transcription and replication, and their links make it easier for the virus to get into cells (Han and Král 2020)

Consequently, it represents a significant objective for the formulation of inhibitory pharmaceuticals for the coronavirus, as agents such as interferon alpha, ribavirin, and lopinavir-ritonavir have been evaluated against the coronavirus proteins (3CLpro) and (RdRp), while favipiravir, mefenovir, cyclophilin, corticosteroids, and alafenamide have been assessed in patients with Middle East Respiratory Syndrome or Severe Acute Respiratory Syndrome, with certain medications remaining contentious despite their efficacy (Al-Masoudi, Elias, and Saeed 2020)

Ran Yu et al. (2020) showed via molecular docking that luteolin exhibits a strong affinity for the coronavirus major protease, contributing significantly to its antiviral efficacy (Yu et al. 2020) . A computational analysis conducted by Jun-Feng Ca et al. (2022) demonstrated that the TMPRSS2 inhibitor efficiently halts coronavirus infection by targeting ACE2, hence inhibiting SARS-CoV-2 infection and facilitating COVID-19 treatment through molecular docking (Cao et al. 2022)

In 2022, Michal Lazniewski et al. used molecular dynamics simulations to find the best drugs to stop the virus from interacting with the ACE2 receptor. They found that zafirlukast and simeprevir were the best inhibitors. (Lazniewski et al. 2022). By using some drugs as anti-coronavirus by targeting the main protein (CLpro3) of the coronavirus, We conducted a multidrug study to analyze their interaction with 3CLpro and their efficacy against SARS-CoV-2 infection using computational methods (Ghosh et al. 2021) .

2 - Methods :

2-1 Density Functional Theory:

Density functional theory calculations were performed using Gaussian 09 program and with the help of Gaussview program, the geometric structures of the studied compounds in the gas phase were optimized using B3LYP function, with the basis set of valence 6-31G(d) (Noureddine, Issaoui, and Al-Dossary 2021) .

2-2 Molecular Docking:

2-2-1 Protein Preparation:

The structure of the main protease of SARS-CoV-2 with N3 inhibitor (PDB ID:6LU7) was obtained from the protein database in pdb format. The 6LU7 protein consists of two chains, A and C, where A acts as a protein and C as a ligand. The A chain was chosen as the core for this. The Chimera program was used (Sumaryada and Pramudita 2021) .To prepare the protein, water molecules and the original ligand were removed, side chains were modified, and hydrogen atoms were added to the crystal structure to ensure that the protein was compatible with docking simulation tools. A relaxation process was also performed (minimization). This file was then

prepared for docking by adding polar hydrogen atoms and charges using AutoDock Tools and saved in the pdbqt extension. (Puthanveedu and Muraleedharan 2022) .

2-2-2 Ligands Preparation:

A comprehensive search was conducted for effective antiviral compounds against a variety of viruses. We collected 50 compounds that had been used to treat the coronavirus (COVID-19) from specialized international journals, including the American Chemical Society. The geometrically optimized compound structures were prepared using Avogadro and saved in PDB file format. The compound files were prepared for molecular docking using AutoDock Tools and saved as files with the PDBQT extension (Al-soud et al. 2021).

2-2-3 Molecular Docking:

Molecular docking was performed using Autodock 4 and Autodock Vina, and grid maps were prepared using Autogrid. The grid size was 6060 x 60 x 100 points, with a grid spacing of 0.375 Å (Banday, Saeed, and Al-Masoudi 2020). The dimensions of the lattice center were x=-12 Å, y=12 Å, and z=68 Å. The resulting molecular docking was visualized using PyMOL (Ghosh et al. 2021).

3 – Results :

3-1 Primary compounds used as synthetic nuclei:

The aim of the study was to design a series of anti-COVID-19 compounds based on compounds effective against this virus. Fourteen compounds with proven efficacy against COVID-19 were selected. The electronic structures of these compounds after geometric optimization using the B3LYP/6-31G(d) level are shown in Figure 1. Its total energies, dipole moments, and the energies of adjacent orbitals (homo and lumo) are also known. The energy differences between them are shown in Table 1, and the shapes of the homo and lumo orbitals are shown in Figure 2.

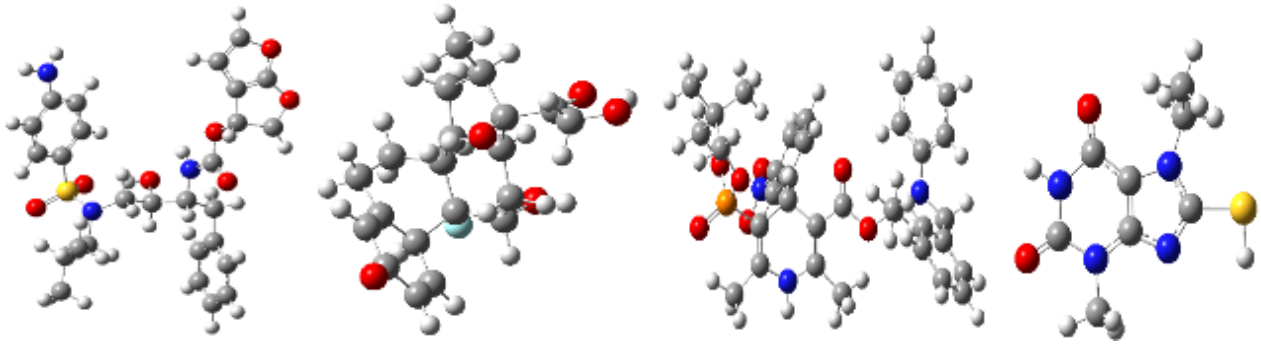

1- darunavir 2- Dexamethasone 3-Efonidipine 4- Emmdpd

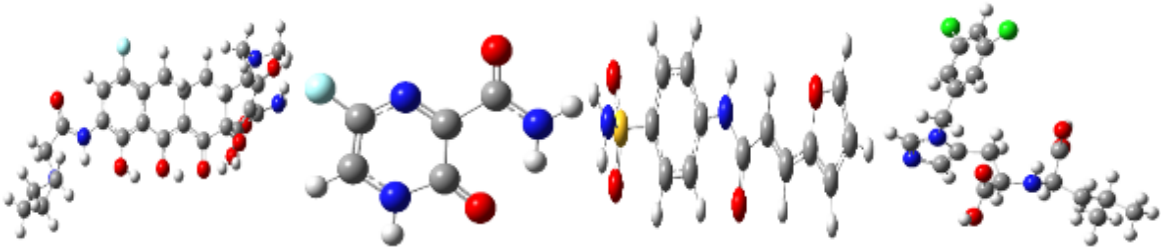

5- Eravacycline 6- Favlplravir 7- FSP 8- HTCC

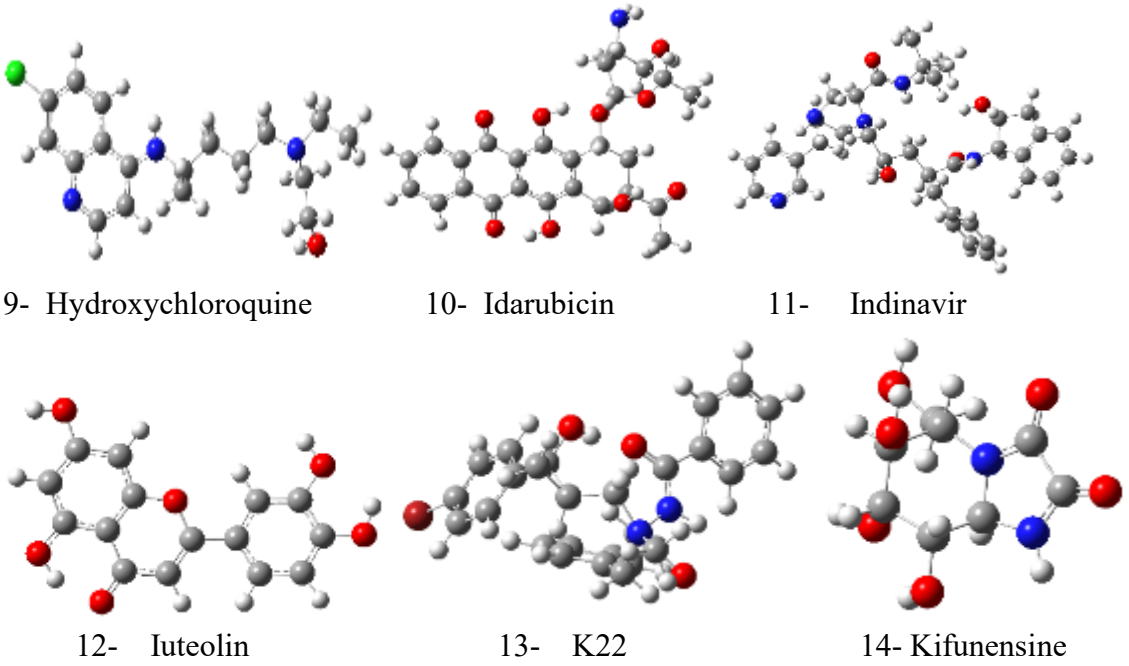

9- Hydroxychloroquine 10- Idarubicin 11- Indinavir

12- Iuteolin 13- K22 14- Kifunensine

Figure 1: Electronic structures of the compounds after geometric optimization using the B3LYP/6-31G(d) level.

Table 1: Total energy, dipole moments, energies of adjacent orbitals (homo and lumo), and energy differences for the studied compounds.

	Ligand	**Total energy**	**HOMO**	**LOMO**	**Energy gap**	**Dipole moment debye**
1	darunavir	-2136.997062	-0.18955	-0.02859	0.16096	6.184270
2	Dexamethasone	-1253.080340	-0.24449	-0.06829	0.17620	4.314264
3	Efonidipine	-2350.653336	-0.18888	-0.07870	0.11018	5.031418
4	Emmdpd	-1078.569997	-0.21596	-0.03354	0.18242	3.904629
5	Eravacycline	-1967.550259	-0.15810	-0.10305	0.05505	9.459553
6	Favlplravir	-607.481725	-0.24666	-0.09768	0.14898	5.905134
7	FSPA	-1311.112155	-0.22328	-0.07313	0.15015	7.331327
8	HTCC	-2123.438192	-0.21896	-0.03137	0.18759	2.536610
9	Hydroxychloroquine	-1401.237311	-0.21019	-0.04440	0.16579	4.878311
10	Idarubicin	-1738.780953	-0.20876	-0.09643	0.11233	3.516529
11	Indinavir	-1974.791531	-0.20498	-0.02632	0.17866	4.533249
12	Iuteolin	-1028.956999	-0.21547	-0.06496	0.15051	4.950594
13	K22	-3952.018009	-0.22373	-0.04617	0.17756	3.160733
14	Kifunensine	-872.894162	-0.24144	-0.03253	0.20891	6.843616

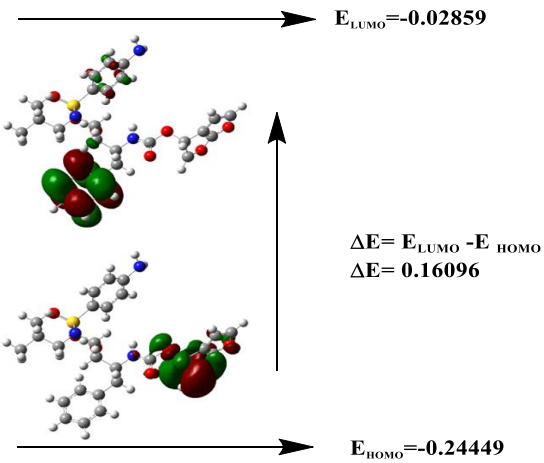

Figher 1: darunavir

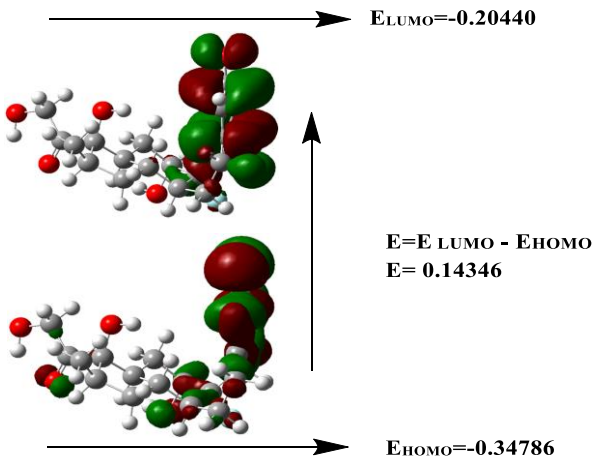

Figher 2 : Dexamethasone

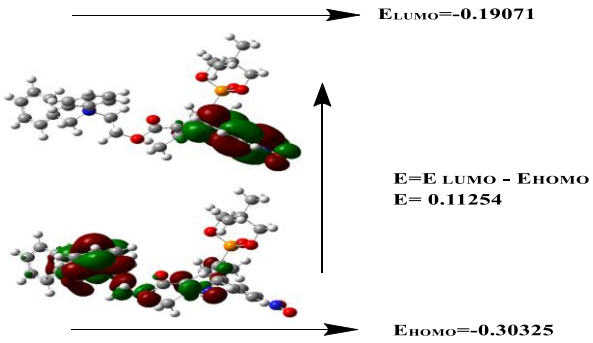

Figher 3 : Efonidipine

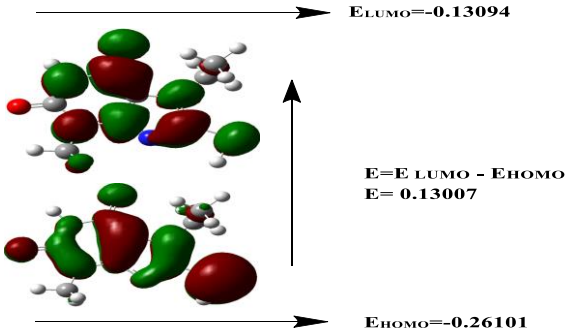

Figher 4 : Emmdpd

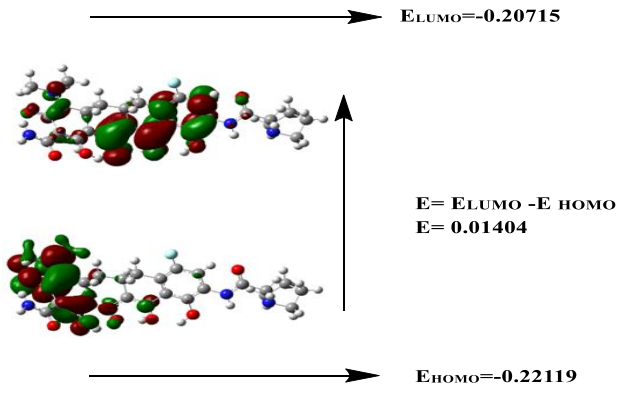

Figher 5 : Eravacycline

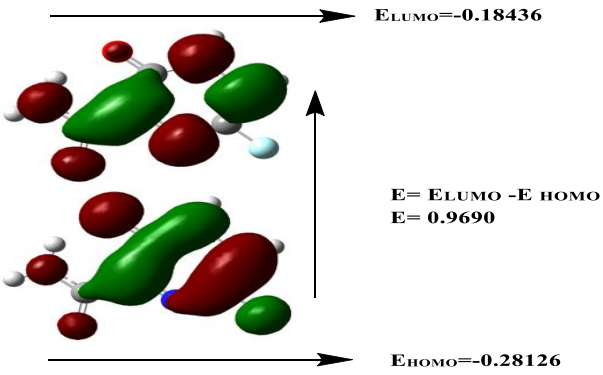

Figher 6 : Favlplravir

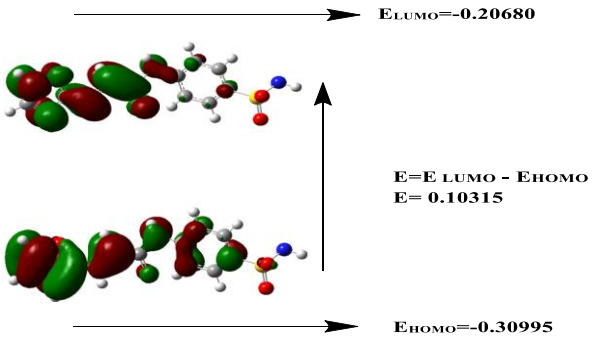

Figher 7 : FSPAD

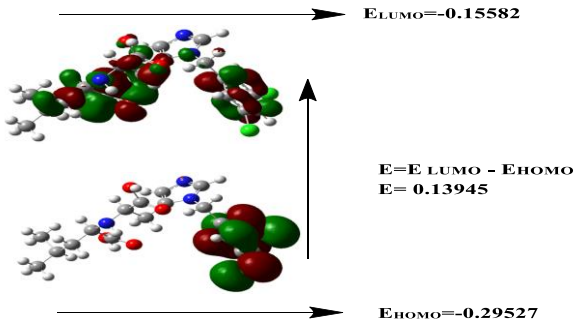

Figher 8 : HTCC

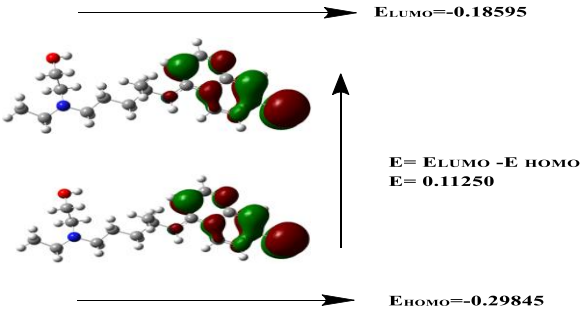

Figher 9 : Hydroxychloroquine

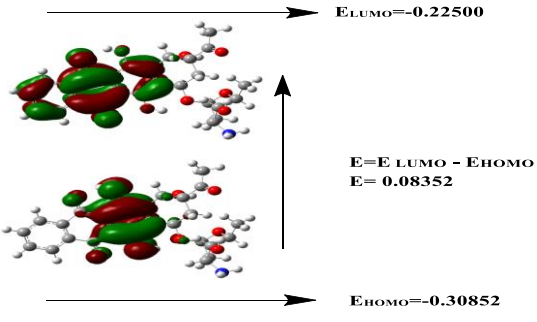

Figher 10 : Idarubicin

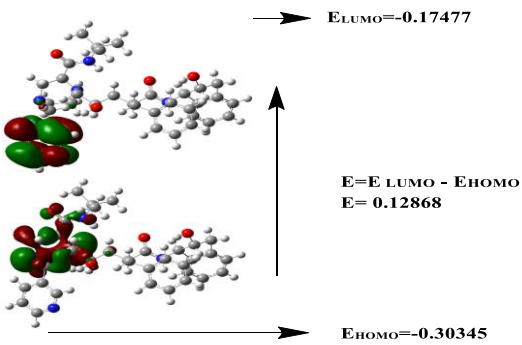

Figher 11: Indinavir

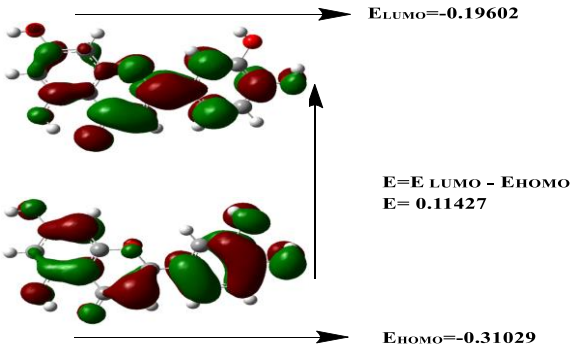

Figher 12: Iuteolin

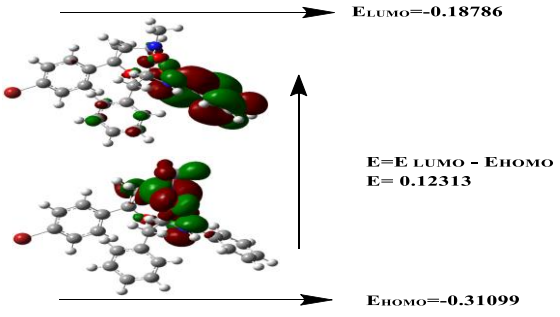

Figher 13: K22

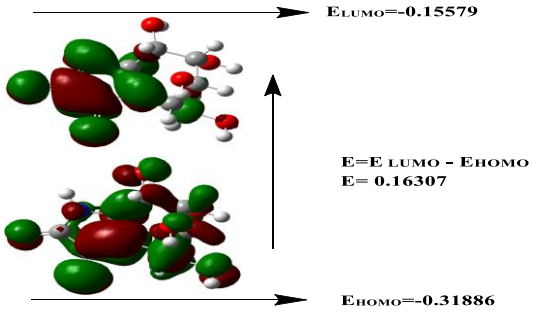

Figher 14: Kifunensine

Figure 2: Homo and homogeneous orbitals of the studied compounds.

In this study, we were unable to establish correlations between the structural properties of the studied compounds and any of the total energy values, dipole moment values, or adjacent orbital energy values This is due to the great variation in their chemical compositions in terms of size, type of atoms, and type of bonds. However, these structures were used for molecular docking calculations and as nuclei for the design of subsequent compounds for study.

3-2 Docking results for initial vehicles:

Molecular docking calculations were performed for the initial compounds (14 compounds) Using AutoDoc-4 and Vina software, we evaluated the theoretical efficacy of these compounds against the 6LU7 protein as a target representing COVID-19 and The results of the docking are shown in Table 2.

It is noted from this table that the calculated binding energies, which represent the activity, range from -4.48 to -12.27 kcal/mol in the case of Autodock-4 and From -4.9 to -8.7 kcal/mol in the case of phenylketonuria. The best four compounds based on the calculated binding energy values are: Emmdpd , Favlplravir , Kifunensine , Hydroxychloroquine which have binding energies of -5.8, -4.9, -6.2 and -6.3 kcal/mol, respectively.

Table 2: Molecular docking results of the initial compounds using AutoDoc-4 and Vina.

	compaund	**vina**	**Auto dock**
1	darunavir	-7.6	-10.13
2	Dexamethasone	-6.5	-8.33
3	Efonidipine	-8.4	-10.84
4	Emmdpd	-5.8	-5.37
5	Eravacycline	-7.7	-11.07
6	Favlplravir	-4.9	-4.48
7	FSPA	-6.7	-7.34
8	HTCC	-7.5	-7.60
9	Hydroxychloroquine	-6.3	-6.99
10	Idarubicin	-8.7	-12.27
11	Indinavir	-7.8	-11.17
12	Iuteolin	-7.5	-8.70
13	K22	-6.8	-11.00
14	Kifunensine	-6.2	-5.96

3-3Designed Vehicles:

The electronic structures obtained previously have been used to construct compounds designed as anti-coronaviruses This is after selecting four compounds that have the highest calculated values of binding energies, which are the compounds shown in Figure 3. The design process involved adding a series of functional groups that have a range of Hammett constant values (Hansch, Leo, and Taft 1991), namely CH_3, NH_2, CHO, Cl, Br, CN, OH, and NHOH, as shown in Table 3.

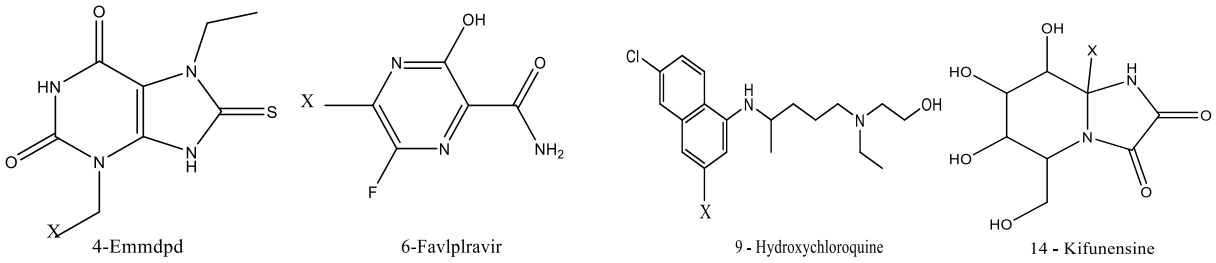

Figure 3: Electronic structures used in building compounds designed as anti-coronavirus.

Table 3: Values of important constants for effective groups.

	Effective groups	Values of hammett constants
1	CH3	-0.17
2	NH2	-0.66
3	CHO	0.42
4	Cl	0.23
5	Br	0.23
6	CN	0.66
7	OH	-0.37
8	NHOH	-0.34

Since the number of added groups was eight, this resulted in the design of thirty-two compounds. These compounds were subjected to geometric optimization using the B3LYP/6-31G(d) level of theory. The values of their total energies, dipole moments, and energies of the filled orbitals are shown in Table 3-4.

Tables 3-4: Energy, HOMO, LOMO, energy difference, dipole moment of the complex Mannostatin and its compensations.

	Ligand	Total energy	HOMO	LUMO	Energy gap	Dipole moment debye
1.	4 a	-1117.886988	-0.21507	-0.03217	0.18290	3.890232
2.	4 b	-1133.913600	-0.21526	-0.03180	0.18346	4.630202
3.	4 c	-1191.881964	-0.22567	-0.04300	0.18267	5.563254
4.	4 d	-1538.163284	-0.22807	-0.04613	0.18194	4.571942
5.	4 e	-3649.672649	-0.22767	-0.04869	0.17898	4.512185
6.	4 f	-1170.800061	-0.22975	-0.04603	0.18372	5.125070

7.	4 g	-1153.783621	-0.22235	-0.03791	0.18444	3.669565
8.	4 h	-1209.074764	-0.21700	-0.03354	0.18346	4.310408
9.	6 a	-646.806344	-0.23915	-0.09158	0.14757	6.585019
10.	6 b	-662.842685	-0.22137	-0.07615	0.14522	8.150282
11.	6 c	-720.796527	-0.26139	-0.13213	0.12926	5.218447
12.	6 d	-1067.071085	-0.25207	-0.10546	0.14661	4.995936
13.	6 e	-3178.580958	-0.25016	-0.10450	0.14566	5.183136
14.	6 f	-699.713671	-0.26760	-0.13270	0.13490	3.622903
15.	6 g	-682.692714	-0.23366	-0.08582	0.14784	7.594690
16.	6 h	-737.991383	-0.23054	-0.08798	0.14256	6.975789
17.	9 a	-1440.558471	-0.20844	-0.04068	0.16776	4.557946
18.	9 b	-1456.602279	-0.20200	-0.03350	0.16850	4.426710
19.	9 c	-1514.554060	-0.21898	-0.07599	0.14299	7.740352
20.	9 d	-1860.837127	-0.21790	-0.05300	0.16490	6.237096
21.	9 e	-3972.345037	-0.21778	-0.05335	0.16443	6.108743
22.	9 f	-1493.477264	-0.21959	-0.07159	0.14800	8.230474
23.	9 g	-1476.470727	-0.21133	-0.04048	0.17085	3.747074
24.	9 h	-1531.760204	-0.20531	-0.03842	0.16738	4.182429
25.	14 a	-912.208472	-0.24256	-0.03350	0.20906	6.595271
26.	14 b	-928.246160	-0.24589	-0.04027	0.20562	5.619309
27.	14 c	-986.203399	-0.25311	-0.06082	0.19229	5.204481
28.	14 d	-1332.487903	-0.26045	-0.06697	0.19348	5.569641
29.	14 e	-3444.002198	-0.26101	-0.07704	0.18397	5.440234
30.	14 f	-965.118893	-0.26019	-0.05261	0.20758	6.016075
31.	14 g	-948.114284	-0.24682	-0.04054	0.20628	6.614922
32.	14 h	-1003.406595	-0.24970	-0.04547	0.20423	5.927533

3-3-1 Verify the feasibility of adding effective groups:

The feasibility of adding functional groups to the original structures was verified through the influence of their adjacent orbitals (homo and luminosity) of the designed compounds on the nature of the added group, expressed by the Hammett constant. These orbitals describe the region between the electron-filled and electron-free states in molecules and they play an essential role in determining the chemical activity of molecules (Venkataramanan et al. 2015).

Figures 4 to 11 show the relationship between the values of the Hammett constants for the substituents and the values of both the homo and lumo of the designed compounds. It is noted that there are correlations that range mostly from acceptable to excellent in the case of the values of homo and lumo energies. In the case of Homo (Figures 4 to 7), the values of the regression constant (R2) ranged between 0.6128 and 0.9889.

The strong correlations in the cases of hydroxychloroquine (0.8781) and favlebletravir (0.9889) provided regression equations with which the homo values of these compounds could be calculated by simply knowing the values of the Hammett constants for the additives. As for the relationship between the values of the Lumo energies and the Hammett constants, the values of the rebound constants ranged between 0.7055 and 0.9162, except for the compound kefunensine, whose rebound constant value was 0.4148. As with homo energies, the derivatives of the compound Pfaffelplerafer have the highest recoil constant values. This can be explained by their aromatic structure, which allows the charge to spread from the added group across the molecular structure by resonance, which in turn is reflected in the orbitals. From these results, it can be concluded that the introduction of additives provides a variety of effectiveness for the designed compounds.

On the other hand, no important relationships were obtained in the case of total energies and values of dipole moments, especially in the case of total energies, due to the difference in molecular weights, which leads to a difference in the number of electrons and thus to a difference in total energies (Barhoumi, Bakkas, and Hajbi 2016).

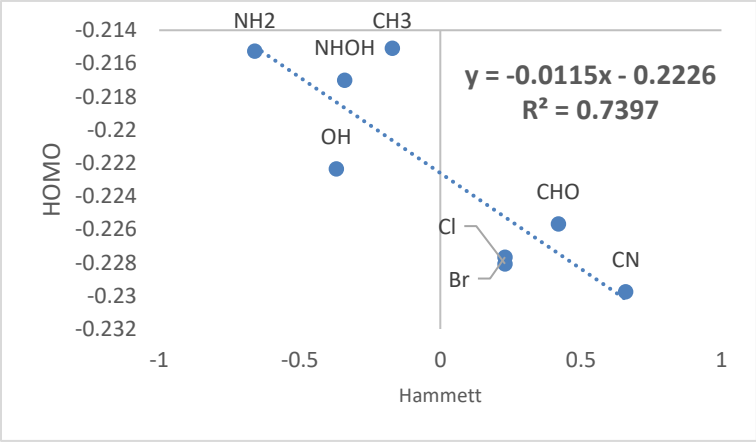

Figure 4: Relationship between the values of Hammett constants for the substituents and the homo values for the 4-component.

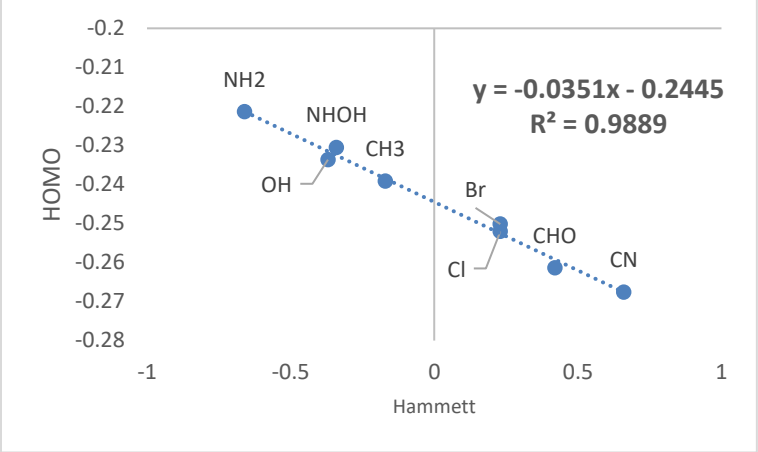

Figure 5: Relationship between the values of Hammett constants for the substituents and the homo values for the 6-component.

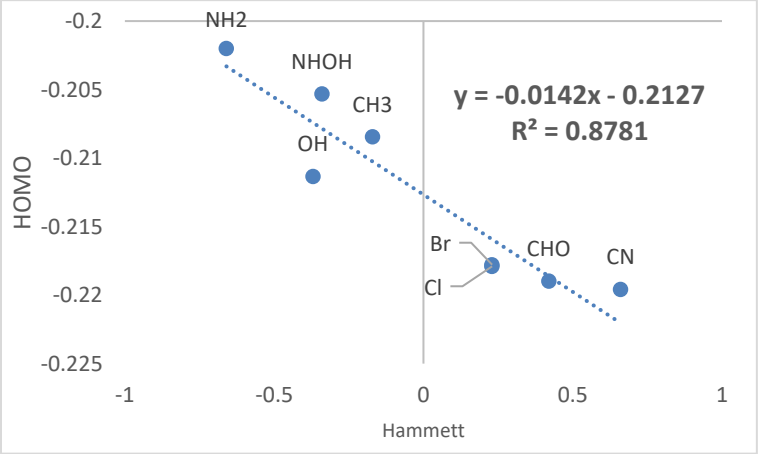

Figure 6: Relationship between the values of Hammett constants for the substituents and the homo values for the 9-component.

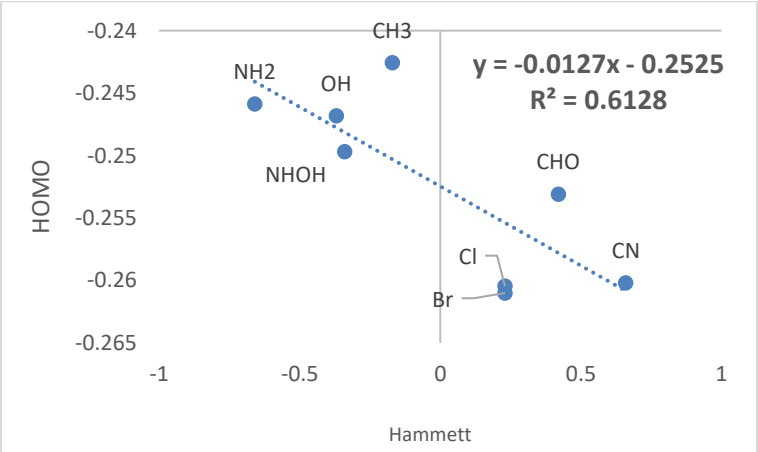

Figure 7: Relationship between the values of Hammett constants for the substituents and the homo values for the 14-component.

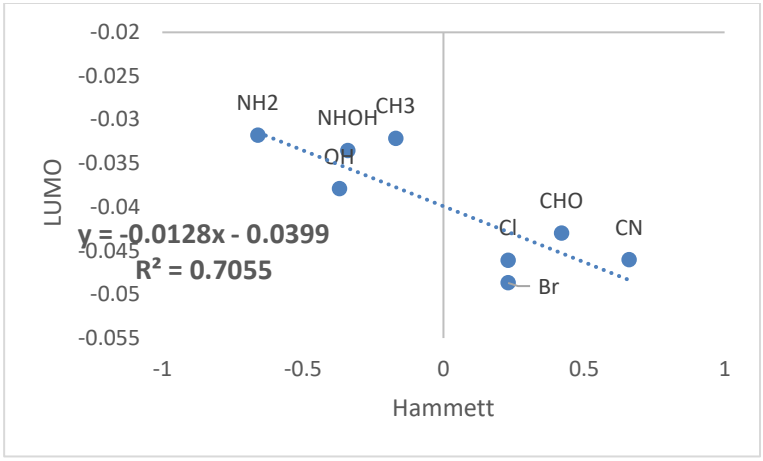

Figure8: Relationship between the values of Hammett constants for the compensators and the values of the lumo for the 4-component .

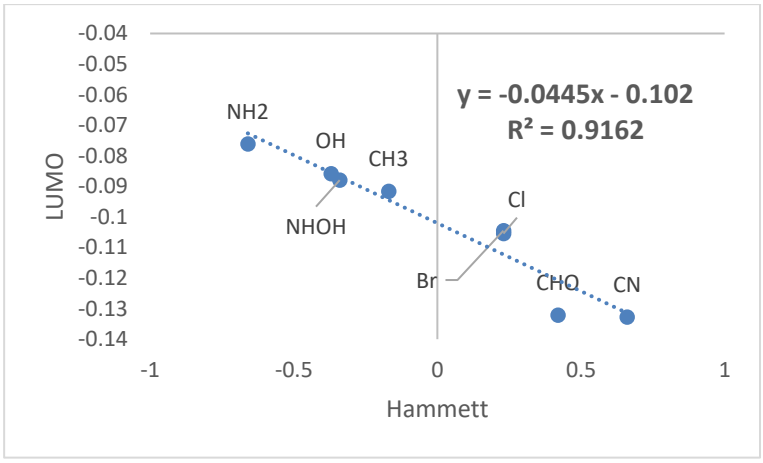

Figure 9: Relationship between the values of Hammett constants for the compensators and the values of the lumo for the 6-component .

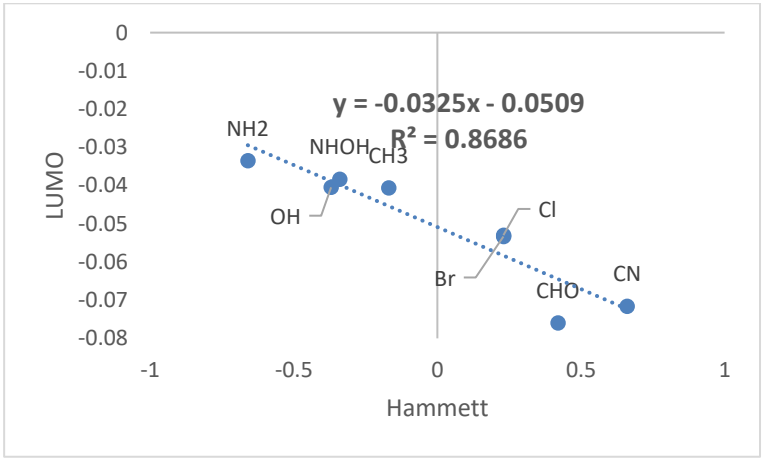

Figure 10: Relationship between the values of Hammett constants for the compensators and the values of the lumo for the 9-component .

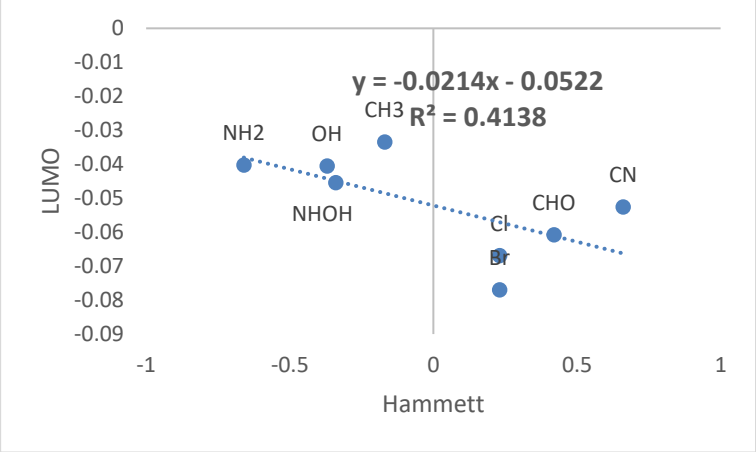

Figure 11: Relationship between the values of Hammett constants for the compensators and the values of the lumo for the 14-component .

3-3-3Molecular docking results of the designed compounds:

Molecular docking of the designed compounds was performed to select the best one. The results of the calculations using the AutoDoc-4 and Vina programs are shown in Table 5. The table shows that the highest calculated values of binding energies for compounds 4h, 6b, 9f and 14h are -6.73, -5.99, -7.88 and -9.76, respectively.

Table 5 : Molecular docking of the Mannostatin complex and its substituents with the major protein (6LU7).

Ligand		Vina	Auto dock
4	4	-5.8	-5.37
	4a	-5.8	-5.50
	4b	-5.7	-5.71
	4c	-5.7	-5.42
	4d	-5.8	-5.37
	4e	-5.8	-5.51
	4f	-6.1	-5.58
	4g	-5.9	-5.46
	4h	-6.2	-5.73
	6	-4.9	-4.48
	6a	-5.3	-4.92
	6b	-6.0	-5.99
	6c	-5.3	-5.5

6	6d	-5.3	-5.03
	6e	-5.3	-5.27
	6f	-5.5	-5.38
	6g	-5.7	-5.44
	6h	-5.6	-5.27
9	9	-6.3	-6.99
	9a	-6.5	-7.65
	9b	-6.6	-6.96
	9c	-6.4	-7.27
	9d	-6.4	-7.77
	9e	-6.5	-7.78
	9f	-6.9	-7.88
	9g	-6.6	-6.93
	9h	-6.8	-7.83
14	14	-6.2	-5.96
	14a	-5.9	-5.75
	14b	-6.3	-8.53
	14c	-5.7	-6.52
	14d	-5.5	-6.12
	14e	-5.4	-6.24
	14f	-5.9	-5.96
	14g	-6.1	-9.47
	14h	-6.4	-9.76

3-3-3-1 Active site of protein 6LU7:

Figure 12 shows the amino acids that form the active site of the target protein 6LU7 with the inhibitor N3 and includes all of the amino acids Thr24, Thr26,His41, Met49, Tyr54, Phe140, Leu141, Asn142, Gly143, Sr144, Cys145, His163, Met165, Glu166, Leu167, Pro168, Asp187, Arg188, Gln189و Thr190, Ala191, Gln192 . The success of molecular docking calculations in including the studied ligand in this site gives a positive indication of the effectiveness of this

ligand as an inhibitor of the virus's activity in the protein (Kim, Grams, and Hsu 2025)(Zheng et al. 2025).

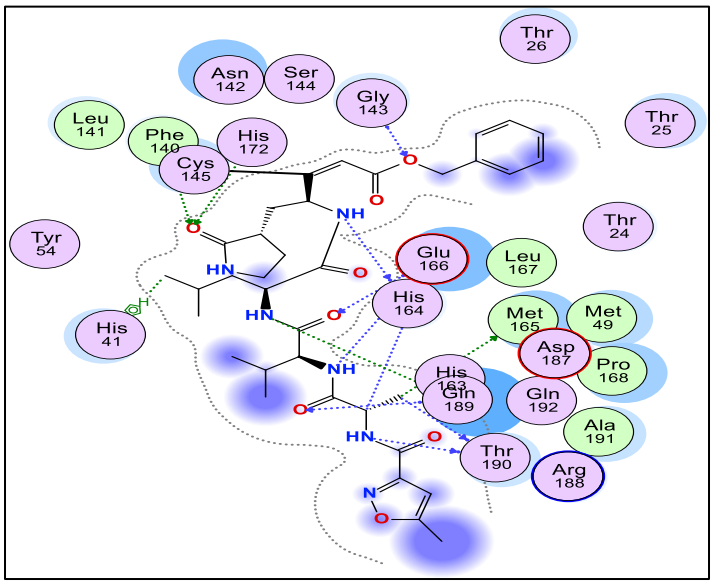

Figure 12: Active site of 6LU7 protein in the presence of inhibitor N3.

3-3-3-2 Results of the docking for the molecules designed in this study:

The results of the docking calculations for the designed vehicles 4h, 6b, 9f, and 14h are shown in Table 6 and Figures 13 to 16.

It is noted from Table 7 that the values of the binding energies between the protein and the ligand for the studied compounds range from -5.99 for compound 6b to -9.76 kcal/mol for compound 14h. They are generally higher than the binding energies calculated for unsubstituted ligands, which indicates that the introduction of substituted groups had a positive effect on the affinity of these ligands for the protein(Nguyen et al. 2020)(Gupta et al. 2022)

As shown in the table, all ligands form hydrogen bonds with various amino acids, with lengths ranging from 2.37 to 4.44 angstroms They have shorter hydrogen bond lengths than the calculated lengths of the 6LU7 protein docking with chloroquine and similar compounds, which were about 5 angstroms (Achutha, Pushpa, and Suchitra 2020).

Based on the study that included solving the crystal structure of the protein 6LU7 , the main residues of the active site of the N3 inhibitor are the amino acid regions His41, Tyr54, Met49, Phe140, Cys145, His163, Pro168, His172, Asp187, Gln192 It is noted from Table 3-8 and Figures 3-27 to 3-36 that all the studied molecules fall within these regions in one way or another, which indicates that they have a behavior similar to the N3 inhibitor in their interaction with the protein.

Table 6: Molecular docking results for compounds 4h, 6b, 9f, and 14h.

No.	Ligand	Binding energy	RMSD	Hydrogen bonding			Active site
				Ligand-receptor interaction	Ligand-receptor Distance	Interaction energy (kcal/mol)	
1	4h	-5.73	1.546	C10 5-ring His41 H-pi 6-ring →CA Gln189 pi-H 6-ring→CG Gln189 pi-H	3.61 4.44 3.57	-1.7 -0.5 -0.7	His41 , Met49, Tyr54 , His164, Met165 , Glu166, Val186 ,Asp187, Arg188, Gln189
2	6b	-5.99	1.096	N10→HIS164	3.54	-0.5	His41, Met49, Tyr54, His164 Met165, Glu166, Asp187, Arg188, Gln189, Thr190, Gln192
3	9f	-7.88	1.552	O21←HIS163	3.09	-2.6	His41, Met49, Tyr54, Phe140, Leu141, Asn142, Gly143, Sr144, Cys145, His163, His164, Met165, Glu166, His172, Asp187, Arg188, Gln189
4	14h	-9.76	0.955	O13→CYS145 O12←HIS163	3.30 2.37	-2.0 -2.0	Leu27, His41, Phe140, Leu141, Asn142, Gly143, Sr144, Cys145, His163, His164, Met165, Glu166, Gln189

3-3-3-3 Root Mean Square Deviation (RMSD) Values:

The root mean square deviation (RMSD) is a number that assesses the accuracy of the binding positions between the protein and the ligand. It is a measure of the average difference in atomic positions between two electronic configurations, which enables an assessment of the extent to which the positions calculated by docking are close to a reference position, which is usually the position represented by the crystal structure. The acceptable value should not exceed 2.5(Castro-Alvarez, Costa, and Vilarrasa 2017). It is noted from Table 7 that the values of the root mean square deviation fall within the range of 0.955 - 1.552 and thus do not exceed the highest permissible value.

4-3-3-3Binding energies:

The calculated binding energies between the designed compounds and the protein are as follows: 14> 9> 6> 4, where the energies were -9.76, -7.88, -5.99, -5.73 kcal/mol, respectively. Energies can be roughly classified into three categories: The first is 9.76 and belongs to molecule 14, the second is 7.88 and belongs to molecule 6. This indicates that the compounds fall into three categories in terms of effectiveness.

Molecule 4 (Figure 13) is characterized by not forming hydrogen bonds but rather Proton-pi bonds, and this may explain its low relative binding energy with the protein.

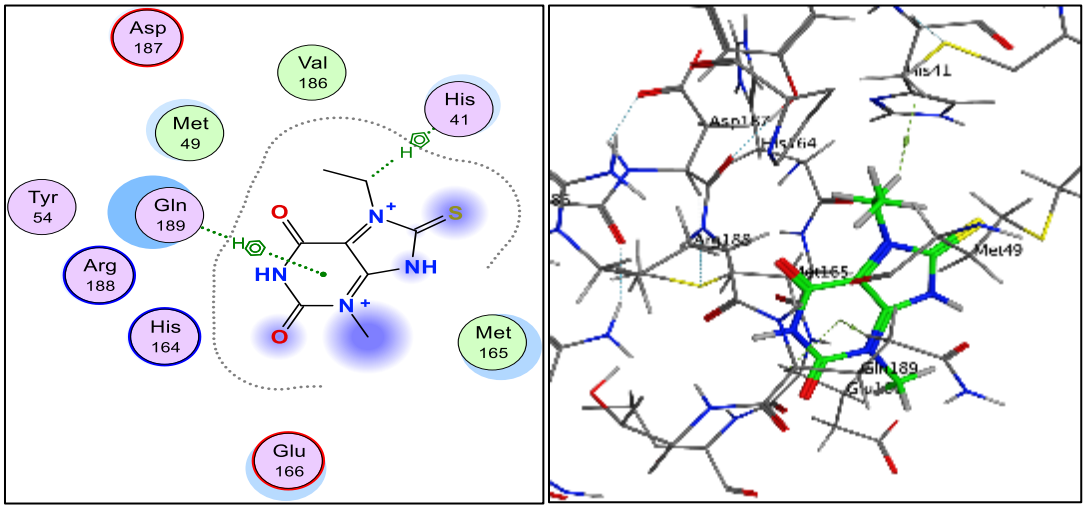

Figure 13: The isomerization of molecule 4h in its complex with 6LU7.

Molecule 6 (Figure 14) has the weakest binding energy and, as a result, the lowest activity, which is represented by its formation of a single hydrogen bond with an energy of -0.5 kcal/mol and a length of 3.54 angstroms, in which it is a proton donor to the acid HIS164.

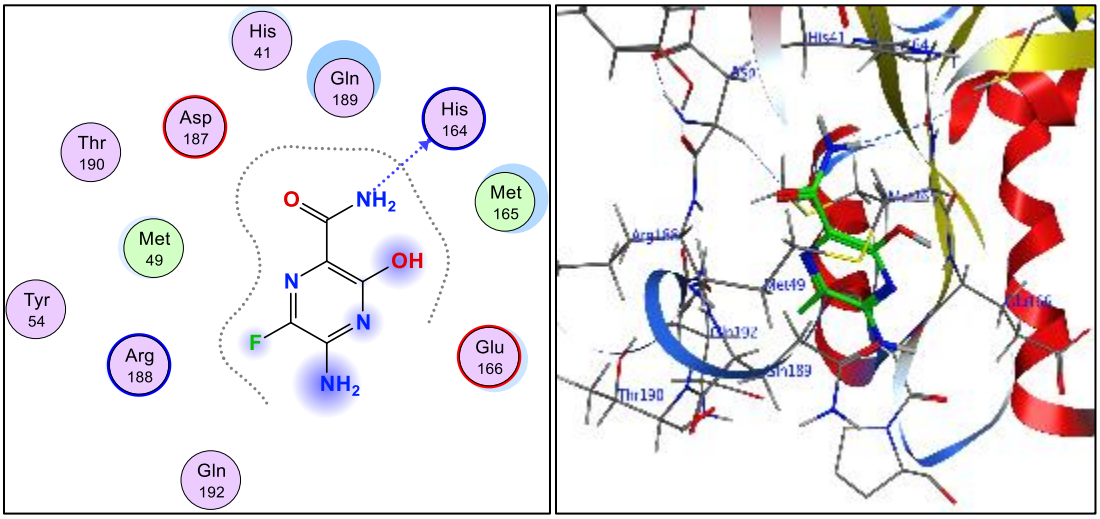

Figure 14: The isomerization of molecule 6b in its complex with 6LU7.

Molecule 9 (Figure 15) falls into the same activity class as molecule 30 and has a binding energy of 7.88 kcal/mol. It is bound to the protein by a single hydrogen bond in which it has

acquired a proton from the amino acid HIS163 via the oxygen atom 21. The preferred hydrogen bond length (3.09 Å) and the relatively high bond energy (2.60 kcal/mol) may be the reason for its relatively high binding energy compared to other molecules.

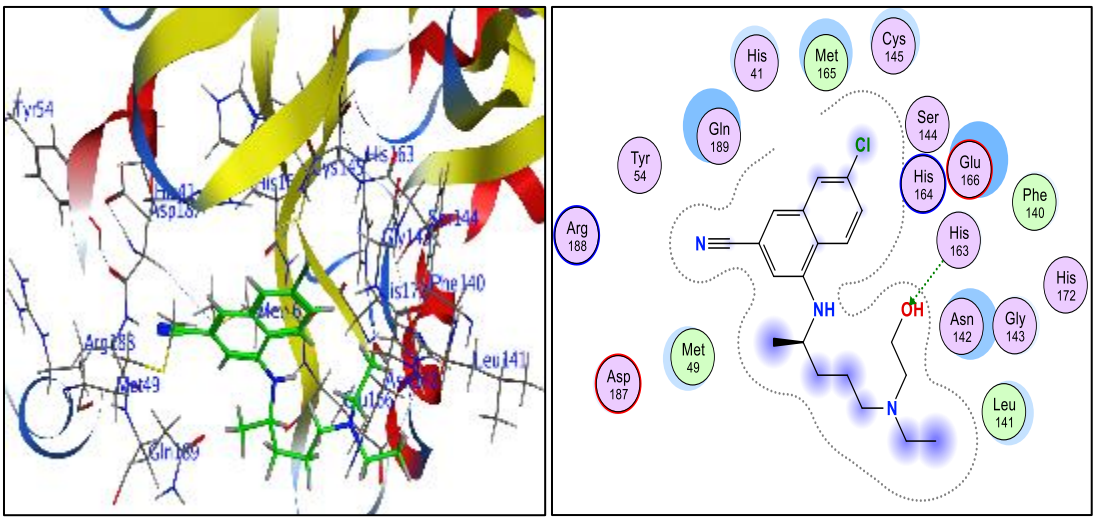

Figure 3-15: The isomerization of molecule 9f in its complex with 6LU7.

Compound 14 (Figure 16) has the highest binding energy with the protein, which could make it the most potent compound in the group. The complex forms two hydrogen bonds with the protein, one of which is a proton donor to the amino acid Cys145 through oxygen atom 13 and has a bond strength of -2.0 kcal/mol, and the second of which is a proton acceptor from the amino acid His163 through oxygen atom 12, and the two bonds have lengths of 3.30 and 2.37 angstroms, respectively.

The relatively high bond energies (2.0 kJ/mol) and the preferred hydrogen bond length O12←HIS163 can explain the relatively high binding energy of this molecule.

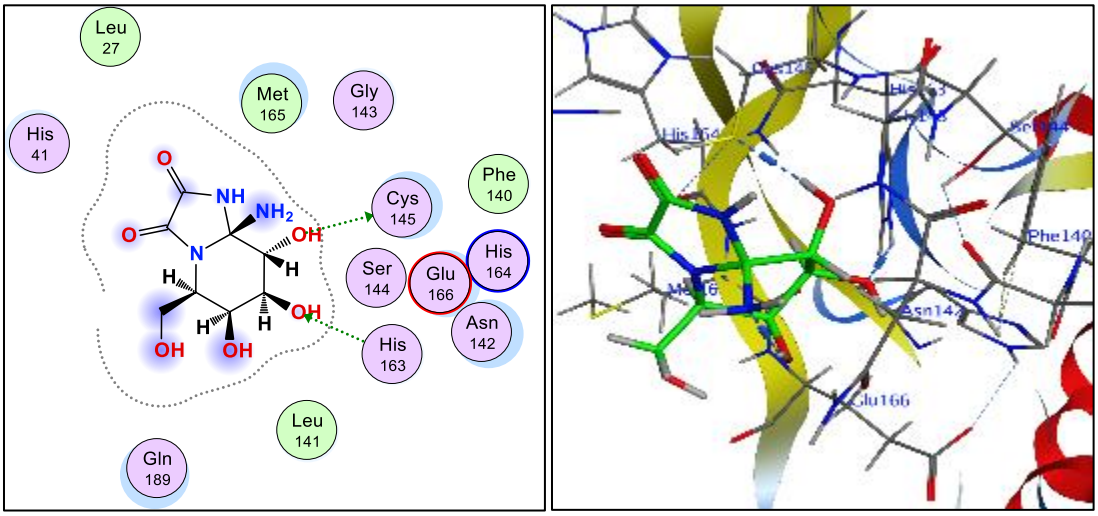

Figure 3-16: The isomerization of molecule 14h in its complex with 6LU7.

4-Conclusions:

In this study, we designed eight eight Emmdpd ,Favlplravir, Hydroxychloroquine and Kifunensine -derived molecules as anti-SARS-CoV-2 inhibitors to evaluate and compare their binding degrees to SARS-CoV 3CLpro enzyme by molecular docking using Autodock Vina and Autodock4 methods. the results showed that the Compounds 4h, 6b, 9f and 14h formed interactions with the main enzyme of the coronavirus, which predicts its potential to become an inhibitor of SARS-CoV-2.

Acknowledgments:

The researcher expresses his gratitude to all his colleagues at the University of Basrah/College of Education for Pure Sciences for their valuable peer review and contributions to enriching his work:

Disclaimer of Conflict of Interest:

The researcher declares that he has no known financial interests or personal relationships that could influence the work presented in this paper.

Reference:

Achutha, A. S., V. L. Pushpa, and Surendran Suchitra. 2020. "Theoretical Insights into the Anti-SARS-CoV-2 Activity of Chloroquine and Its Analogs and in Silico Screening of Main Protease Inhibitors." *Journal of Proteome Research* 19 (11): 4706–17. Theoretical Insights into the Anti-SARS-CoV-2 Activity of Chloroquine and Its Analogs and In Silico Screening of Main Protease Inhibitors | Journal of Proteome Research

Al-Masoudi, Najim A., Rita S. Elias, and Bahjat Saeed. 2020. "Molecular Docking Studies of Some Antiviral and Antimalarial Drugs via Bindings to 3cl-Protease and Polymerase Enzymes of the Novel Coronavirus (Sars-Cov-2)." *Biointerface Research in Applied Chemistry* 10 (5): 6444–59. 2069583710564446459-libre.pdf

Al-soud, Yaseen A, Bahjat Saeed, Luay Abu-qatouseh, and Hossam Al-suod. 2021. "Synthesis , Anticancer Activity and Molecular Docking Studies of New 4- Nitroimidazole Derivatives," no. July. doi: 10.24820/ark.5550190.p011.479.

Baig, Abdul Mannan, Areeba Khaleeq, Usman Ali, and Hira Syeda. 2020. "Evidence of the COVID-19 Virus Targeting the CNS: Tissue Distribution, Host-Virus Interaction, and Proposed Neurotropic Mechanisms." *ACS Chemical Neuroscience*. Evidence of the COVID-19 Virus Targeting the CNS: Tissue Distribution, Host–Virus Interaction, and Proposed Neurotropic Mechanisms | ACS Chemical Neuroscience

Banday, Abid H., Bahjat A. Saeed, and Najim A. Al-Masoudi. 2020. "Synthesis, Aromatase Inhibitory, Antiproliferative and Molecular Modeling Studies of Functionally Diverse D-Ring Pregnenolone Pyrazoles." *Anti-Cancer Agents in Medicinal Chemistry* 21 (13): 1671–79. Synthesis, Aromatase Inhibitory, Antiproliferative and Molecular ...: Ingenta Connect

Barhoumi, Ali, Salem Bakkas, and Abdeslam El Hajbi. 2016. "Theoretical Study of the Regioselectivity of the Reaction between Tetrachloromethane and Trivalent Phosphorus Derivatives Using the DFT B3LYP / 6-31G (d) Method Abstract :" 3: 639–50. Theoretical

study of the regioselectivity of the reaction between tetrachloromethane and trivalent phosphorus derivatives using the DFT B3LYP/6-31G(d) method | Moroccan Journal of Chemistry

Buonaguro, Luigi, Maria Tagliamonte, Maria Lina Tornesello, and Franco M. Buonaguro. 2020. "SARS-CoV-2 RNA Polymerase as Target for Antiviral Therapy." *Journal of Translational Medicine* 18 (1): 1–8. SARS-CoV-2 RNA polymerase as target for antiviral therapy | Journal of Translational Medicine

Cao, Jun Feng, Yunli Gong, Mei Wu, Xingyu Yang, Li Xiong, Shengyan Chen, Zixuan Xiao, et al. 2022. "Exploring the Mechanism of Action of Licorice in the Treatment of COVID-19 through Bioinformatics Analysis and Molecular Dynamics Simulation." *Frontiers in Pharmacology* 13 (September): 1–17. Frontiers | Exploring the mechanism of action of licorice in the treatment of COVID-19 through bioinformatics analysis and molecular dynamics simulation

Castro-Alvarez, Alejandro, Anna M. Costa, and Jaume Vilarrasa. 2017. "The Performance of Several Docking Programs at Reproducing Protein-Macrolide-like Crystal Structures." *Molecules* 22 (1). The Performance of Several Docking Programs at Reproducing Protein–Macrolide-Like Crystal Structures

Collins, Sean P, Alan Storrow, Dandan Liu, Cathy A Jenkins, Karen F Miller, Christy Kampe, and Javed Butler. 2021. "No Title 済無No Title No Title No Title." Assessment of the Lysozyme and Lactoferrin in the Saliva of Vaccinated Individuals against COVID-19 | (Humanities, social and applied sciences) Misan Journal of Academic Studies

Demsa, Simbolon, Setia Agustina, Sembiring christina Anita, and Wahyudi Anang. 2021. "**済無** No Title No Title No Title." *Continum of Care Pada Ibu Dengan Anak Stunting Dan Perilaku Kunjungan Posyandu Balita Pada Masa Pandemi Covid-19* 13 (April): 1–11. Hematological and biochemical parameters changes associated with Coronavirus Disease (COVID-19) for some patients in Missan Province | (Humanities, social and applied sciences) Misan Journal of Academic Studies

Elfiky, Abdo A. 2020. "Anti-HCV, Nucleotide Inhibitors, Repurposing against COVID-19." *Life Sciences* 248 (February). Anti-HCV, nucleotide inhibitors, repurposing against COVID-19 - ScienceDirect

Ghosh, Rajesh, Ayon Chakraborty, Ashis Biswas, and Snehasis Chowdhuri. 2021. "Evaluation of Green Tea Polyphenols as Novel Corona Virus (SARS CoV-2) Main Protease (Mpro) Inhibitors–an in Silico Docking and Molecular Dynamics Simulation Study." *Journal of Biomolecular Structure and Dynamics* 39 (12): 4362–74. Evaluation of green tea polyphenols as novel corona virus (SARS CoV-2) main protease (Mpro) inhibitors – an in silico docking and molecular dynamics simulation study: Journal of Biomolecular Structure and Dynamics: Vol 39, No 12

Gupta, Anamika, Safia Iqbal, Roohi, Mohd Kamil Hussain, Mohd Rehan Zaheer, and Krapa Shankar. 2022. "Visible Light-Promoted Green and Sustainable Approach for One-Pot

Synthesis of 4,4'-(Arylmethylene)Bis(1H-Pyrazol-5-Ols), in Vitro Anticancer Activity, and Molecular Docking with Covid-19 Mpro." *ACS Omega* 7 (38): 34583–98. Visible Light-Promoted Green and Sustainable Approach for One-Pot Synthesis of 4,4'-(Arylmethylene)bis(1H-pyrazol-5-ols), In Vitro Anticancer Activity, and Molecular Docking with Covid-19 Mpro | ACS Omega

Han, Yanxiao, and Petr Král. 2020. "Computational Design of ACE2-Based Peptide Inhibitors of SARS-CoV-2." *ACS Nano* 14 (4): 5143–47. Computational Design of ACE2-Based Peptide Inhibitors of SARS-CoV-2 | ACS Nano

Hansch, Corwin, A. Leo, and R. W. Taft. 1991. "A Survey of Hammett Substituent Constants and Resonance and Field Parameters." *Chemical Reviews* 91 (2): 165–95. A survey of Hammett substituent constants and resonance and field parameters | Chemical Reviews

Kim, Gibae, R. Justin Grams, and Ku Lung Hsu. 2025. "Advancing Covalent Ligand and Drug Discovery beyond Cysteine." *Chemical Reviews*. Advancing Covalent Ligand and Drug Discovery beyond Cysteine | Chemical Reviews

Lazniewski, Michal, Doni Dermawan, Syahrul Hidayat, Muchtaridi Muchtaridi, Wayne K. Dawson, and Dariusz Plewczynski. 2022. "Drug Repurposing for Identification of Potential Spike Inhibitors for SARS-CoV-2 Using Molecular Docking and Molecular Dynamics Simulations." *Methods* 203 (November 2021): 498–510. Drug repurposing for identification of potential spike inhibitors for SARS-CoV-2 using molecular docking and molecular dynamics simulations - ScienceDirect

Li, Guangdi, and Erik De Clercq. 2020. "Therapeutic Options for the 2019 Novel Coronavirus (2019-NCoV)." *Nature Reviews. Drug Discovery* 19 (3): 149–50. Therapeutic options for the 2019 novel coronavirus (2019-nCoV)

Nguyen, Hoang Linh, Nguyen Quoc Thai, Duc Toan Truong, and Mai Suan Li. 2020. "Remdesivir Strongly Binds to Both RNA-Dependent RNA Polymerase and Main Protease of SARS-COV-2: Evidence from Molecular Simulations." *Journal of Physical Chemistry B* 124 (50): 11337–48. Remdesivir Strongly Binds to Both RNA-Dependent RNA Polymerase and Main Protease of SARS-CoV-2: Evidence from Molecular Simulations | The Journal of Physical Chemistry B

Noureddine, Olfa, Noureddine Issaoui, and Omar Al-Dossary. 2021. "DFT and Molecular Docking Study of Chloroquine Derivatives as Antiviral to Coronavirus COVID-19." *Journal of King Saud University - Science* 33 (1): 101248. DFT and molecular docking study of chloroquine derivatives as antiviral to coronavirus COVID-19 - ScienceDirect

Pal, Mahendra, Gemechu Berhanu, Chaltu Desalegn, and Venkataramana Kandi. 2020. "Severe Acute Respiratory Syndrome Coronavirus-2 (SARS-CoV-2): An Update." *Cureus* 2 (3): 1–9. 1612429993-1612429990-20210204-30437-989nfu.pdf

Puthanveedu, Vinduja, and Karuvanthodi Muraleedharan. 2022. "Phytochemicals as Potential Inhibitors for COVID-19 Revealed by Molecular Docking, Molecular Dynamic Simulation and DFT Studies." *Structural Chemistry* 33 (5): 1423–43. Phytochemicals as potential inhibitors

for COVID-19 revealed by molecular docking, molecular dynamic simulation and DFT studies | Structural Chemistry

Sumaryada, Tony, and Cindy Agnitya Pramudita. 2021. "Molecular Docking Evaluation of Some Indonesian's Popular Herbals for a Possible Covid-19 Treatment." *Biointerface Research in Applied Chemistry* 11 (3): 9827–35. 20695837113.98279835-libre.pdf

Venkataramanan, Natarajan Sathiyamoorthy, Ambigapathy Suvitha, Hiroshi Mizuseki, and Yoshiyuki Kawazoe. 2015. "Computational Study on the Interactions of Mustard Gas with Cucurbituril Macrocycles." *International Journal of Quantum Chemistry* 115 (21): 1515–25. Computational study on the interactions of mustard gas with cucurbituril macrocycles - Venkataramanan - 2015 - International Journal of Quantum Chemistry - Wiley Online Library

Yu, Ran, Liang Chen, Rong Lan, Rong Shen, and Peng Li. 2020. "International Journal of Antimicrobial Agents Computational Screening of Antagonists against the SARS-CoV-2 (COVID-19) Coronavirus by Molecular Docking." *International Journal of Antimicrobial Agents* 56 (2): 106012. Computational screening of antagonists against the SARS-CoV-2 (COVID-19) coronavirus by molecular docking - ScienceDirect

Zheng, Yuzhou, Tangrong Wang, Jiaxin Zhang, Sen Wei, Zhijing Wu, Jiali Li, Beihao Shi, Zixuan Sun, Wenrong Xu, and Jian Zhu. 2025. "Plant-Derived Nanovesicles : A Promising Frontier in Tissue Repair and Antiaging." Plant-Derived Nanovesicles: A Promising Frontier in Tissue Repair and Antiaging | Journal of Agricultural and Food Chemistry